Effect of Wall Roughness on Convective Heat Transfer in Commercial Pipes

J. W. SMITH and NORMAN EPSTEIN

University of British Columbia, Vancouver, British Columbia

Heat transfer and fluid friction measurements were made for air flow through a smooth copper pipe and six other commercial pipes, with a ratio of diameter to equivalent sand roughness varying from 640 to 64. The Reynolds number range was 10,000 to 80,000. Though some increase in heat transfer coefficients with roughness was found, the heat transmission per unit power loss always decreased.

The momentum–heat-transfer analogies of Reynolds and Colburn are shown to be inadequate for handling the experimental data. Those of Prandtl and Taylor, von Kármán, and Pinkel fail to show a required Reynolds number dependence of j_h when friction factor has become independent of Reynolds number for a rough pipe. Martinelli's equation shows such dependence and, even in approximate form, gives good prediction of the experimental results.

Although the effect of wall roughness on fluid friction in pipes has received extensive study, investigation of the corresponding effect on convective heat transfer has been restricted to artificially roughened pipes (*7, 8, 25*). Published studies by Cope (*7*) and Sams (*25*), the latter summarized by Pinkel (*21*), at Reynolds numbers exceeding 2,000 indicated that the increase in heat transfer due to machined roughness elements on the inside of tubes is considerably smaller than the accompanying increase in frictional pressure drop for the same fluid velocity. Furthermore, for a given pressure drop roughened pipes showed smaller heat-transmission rates than smooth tubes, and this was also true if the comparison was made for equal power consumption. Apparently the form drag caused by machined roughness projections produces an inefficient type of turbulence from the heat transfer point of view.

The foregoing two studies, however, also indicated that the shape and configuration of the roughness projections are as important as the height of these projections in determining their effect on fluid friction and heat transfer. Moreover, Colburn (*5*) and later Pratt (*23*) analyzed data on metallic turbulence promoters placed within pipes (*14, 19*) to show that in certain instances the heat-transmission performance for a given power loss is increased by such promoters, and Drexel and McAdams (*10*) have shown similar results for wavy surfaces. This leaves open the possibility that for wall roughness as found in commercial pipes the large frictional pressure-drop increase over that for smooth tubes is accompanied by a substantial increase in convective heat transfer. In the present work seven commercial pipes were investigated, covering a large range of roughness ratio D/e.

EXPERIMENTAL APPARATUS AND PROCEDURE

A horizontal double-pipe heat exchanger, illustrated in Figure 1, was used for making the experimental measurements. A controlled and orifice-metered air flow through the inside of the test pipe was heated by pressure-regulated 20 lb./sq. in. gauge saturated steam condensing on the outside of the pipe. To eliminate the steam-film heat transfer resistance, the outside of the test pipe was polished on an emery sander and frequently coated with oleic acid, thus ensuring that condensation of the steam as drops, rather than as a continuous film, always prevailed. This procedure was visually observed by placing the test pipe in a glass tube, into which steam was admitted, before and after the pipe was placed in the experimental steam jacket. Since the test pipes were all new, clean, scale-free, and metallic, no pretreatment was given the inside of the pipes and it was assumed that the only appreciable resistance to heat transfer was in the air film. The measured steam temperature was therefore taken as the temperature of the inside pipe surface.

The orifice assembly, with *vena contracta* taps, was constructed according to A.S.M.E.

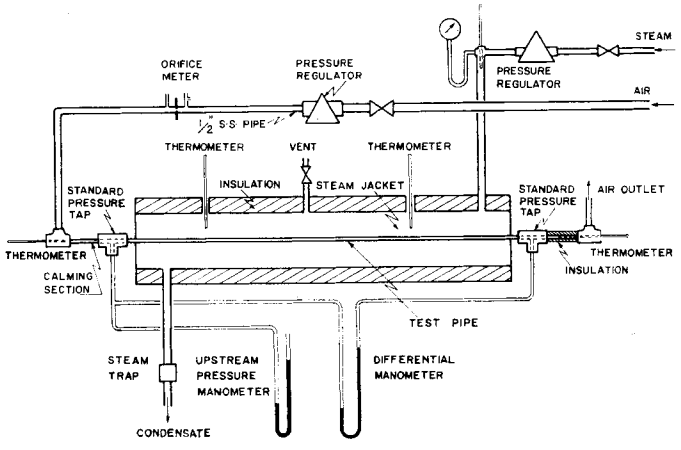

Fig. 1. Schematic diagram of apparatus.

J. W. Smith is at present with DuPont of Canada Ltd., Kingston, Ontario.

specifications (*1*), as were the static pressure taps at the entrance and exit of the test pipes. The bore of the taps was made to conform as closely as possible to the actual inside diameter of the pipe in which they were placed. Orifice plates were calibrated against a diaphragm gas meter. Calibrated thermometers were used to measure inlet-air temperature to 0.1°F., mixed-outlet-air temperature to 0.2°F., and steam temperature to 0.2°F. The steam jacket was vented to ensure release of noncondensables. Pressure drop and upstream pressure manometers were filled with water, carbon tetrachloride, or mercury, depending on the flow rate.

A calming length of 8 in., corresponding to 16–30 inside diameters for the pipes, preceded the heat exchange section. Since L/D of the test pipes was in the range 124–231, this length was, according to Latzko (*16*) and Boelter et al. (*3*) as summarized by McAdams (*18*), sufficient to reduce entrance effects to negligible proportions. A 4-in. unheated mixing section followed the heater, the mixing being accentuated by the fact that the exit thermometer bulb itself was only a little smaller than the small pipe diameters investigated. The heated length of pipe was 5.17 ft. and the distance between pressure taps was 5.55 ft. The seven pipes investigated, together with their inside diameters, are listed in Table 1.

Eighty nonheating and a similar number of heating runs were performed on the pipes. Barometer, manometer, and thermometer readings were recorded at the steady state, which was maintained for at least 15 min. A Reynolds number range of 10,000 to 80,000 was covered. For three of the runs the inlet steam was carefully dried and the condensate from the steam trap was carefully collected through a water-cooled condenser, so that an energy balance might be made on the system.

Data Processing

In all calculations the inside diameter of a pipe was taken as that specified by the manufacturer. Caliper measurements confirmed this assumption. As a further check, the diameter of the ¼-in. standard steel pipe was measured by volumetric displacement of mercury, the deviation of this value from that of the manufacturer being only 0.5%.

For both heating and nonheating runs the frictional pressure drop was related to the measured pressure drop by the following form of the Bernoulli equation for a horizontal pipe:

$$\Delta p_{fr} = p_1 - p_2 - \frac{G^2(v_2 - v_1)}{g_c} \qquad (1)$$

For the nonheating runs the temperature change through the test section rarely exceeded 3°F. and was usually much less. These runs were therefore treated as isothermal at the average air temperature and the data used to calculate the conventional Reynolds number and Fanning friction factor. Correlation of the rough pipe data was achieved by means of Colebrook's (*6*) equation for sand-roughened pipes in the transitional

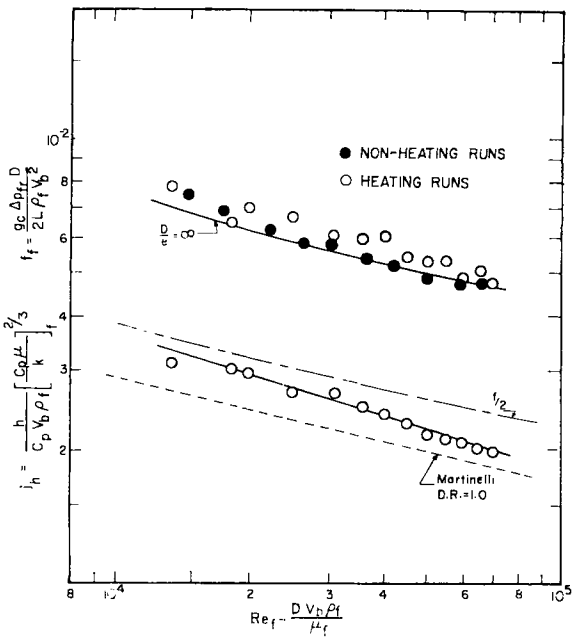

Fig. 2. Copper pipe, 1/4 in.; fluid friction and heat transfer data.

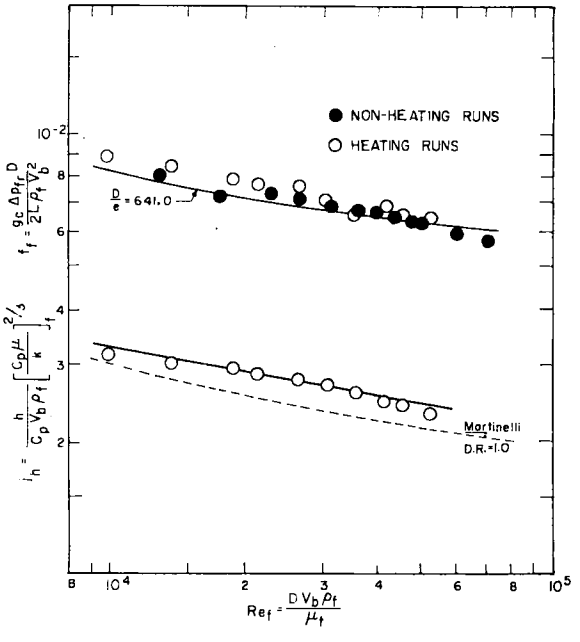

Fig. 3. Standard steel pipe, 3/8 in.; fluid friction and heat transfer data.

Table 1. Properties and Empirical Constants for Various Pipes*

Pipe	D, ft.	D/e, Eq'n. (2)	a, Eq'n. (7)	n, Eq'n. (7)	a.d., %
¼-in. Copper	0.0313	—	0.0585	0.302	±2.1
⅜-in. Standard steel	0.0411	641 ± 32	0.0175	0.183	±1.8
¼-in. Standard steel	0.0303	463 ± 51	0.0365	0.257	±3.2
⅜-in. Galvanized	0.0411	211 ± 12	0.0218	0.205	±1.5
½-in. Karbate	0.0417	189 ± 6	0.0258	0.209	±1.0
¼-in. Galvanized	0.0303	112 ± 2.5	0.0142	0.156	±3.7
⅛-in. Galvanized	0.0224	63.4 ± 1.8	0.00611	0.0714	±3.8

*Complete tabular data are on file as document 5213 with the American Documentation Institute, Photoduplication Service, Library of Congress, Washington 25, D. C., for $2.50 for photoprints or $1.75 for 35-mm. microfilm.

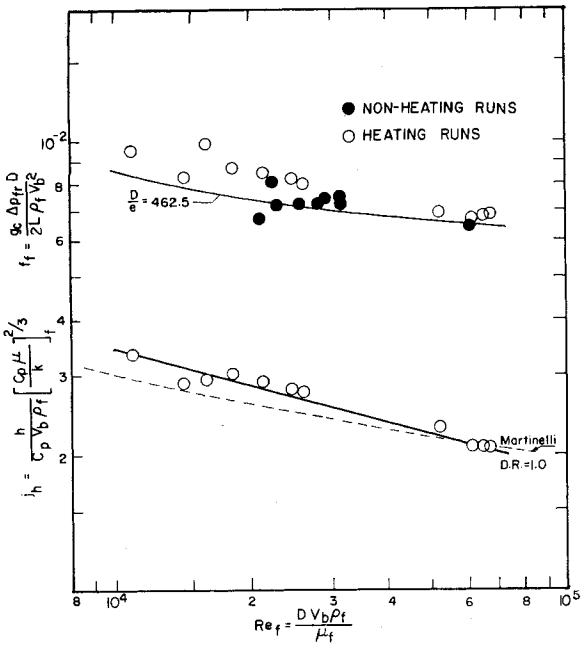

Fig. 4. Standard steel pipe, 1/4 in.; fluid friction and heat transfer data.

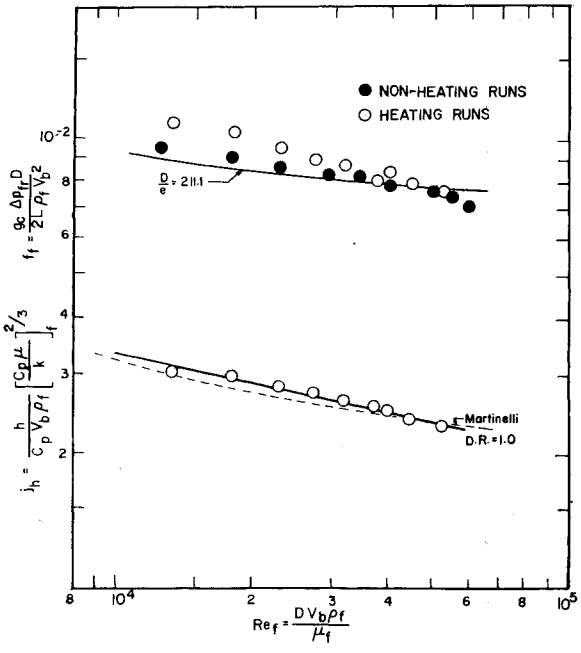

Fig. 5. Galvanized pipe, 3/8 in.; fluid friction and heat transfer data.

region between laminar and completely turbulent flow:

$$\frac{1}{\sqrt{f}} = 4 \log (D/e) + 2.28 - 4 \log \left(1 + \frac{4.67 D/e}{Re\sqrt{f}}\right) \qquad (2)$$

which reduces to the von Kármán-Nikuradse (*12, 20*) equation for rough pipes when turbulence is fully developed. The geometric mean value of the ratio D/e, as calculated from Equation (2), was determined for each rough pipe and is recorded in Table 1, in conjunction with the corresponding "probable error of the mean" (*27*). Correlation of the data for the smooth copper pipe, however, could not be achieved by Equation (2), and therefore these data were handled by the von Kármán-Nikuradse (*12, 20*) equation for smooth tubes:

$$\frac{1}{\sqrt{f}} = 4.0 \log Re\sqrt{f} - 0.40 \qquad (3)$$

Physical properties of air were those used in several N.A.C.A. reports (*11, 25, 29*).

Fluid friction data for the heating runs were correlated, after Humble, Lowdermilk, and Desmon (*11*), by evaluating all fluid properties at the film temperature t_f, defined as midway between the average bulk temperature t_b and the inside wall temperature t_s. The film Reynolds number is defined by

$$Re_f = \frac{DV_b\rho_f}{\mu_f} \qquad (4)$$

and the film Fanning friction factor by

$$f_f = \frac{\Delta p_{fr} D g_c}{2L\rho_f V_b^2} \qquad (5)$$

Humble et al. found that heating data correlated in this manner lay on the curve representing isothermal data, except at Re_f less than 20,000, where the method appeared to overcompensate for radial temperature gradients.

The three energy-balance runs showed an average excess of less than 5% heat lost by the steam over that gained by the air. This was accounted for by heat loss to the surroundings through the insulation. Since the kinetic energy increase of the air was negligible in relation to the enthalpy increase, the heat transfer coefficients were based on the rate of enthalpy increase of the air. Logarithmic mean terminal temperature difference was used in evaluating h.

The heat transfer data were correlated by the film Reynolds number, defined by Equation (4), and the j_h factor of Colburn (4), modified according to the method of Humble et al. (*11*):

$$j_h = \frac{h}{C_p V_b \rho_f} \left(\frac{C_p u}{k}\right)_f^{2/3} \qquad (6)$$

The film Prandtl number for the heating runs deviated little from 0.69. The two dimensionless groups were related by equations of the form

$$j_h = aRe_f^{-n} \qquad (7)$$

The constants a and n, evaluated by the method of least squares, are listed in Table 1 for the various pipes. The average deviation (*a.d.*) of j_h calculated by these equations from the measured values of j_h is also recorded in Table 1 for each pipe.

SUMMARY AND INTERPRETATION OF RESULTS

The processed fluid friction and heat transfer data for the various pipes are plotted in the form of dimensionless groups in Figures 2 through 8. The curve through the friction-factor points for the copper pipe is based upon Equation (3), and the friction-factor curves for the other pipes are based on Equation (2), the geometric mean value of D/e calculated from the nonheating data being used. In accordance with Humble et al. (*11*), the correlation of the heating data,

using film Reynolds number and friction factor, with the nonheating data, is better at high than at low Reynolds numbers, where film friction factors for heating tend to exceed isothermal friction factors. The agreement is good, nevertheless, and shows that no significant changes occurred in the pipe surfaces in the intervals between nonheating and heating runs.

The solid lines through the heat transfer points are plotted according to Equation (7), with the constants as determined by least squares. For purposes of comparison, all the curves, without the corresponding data points, are replotted in Figure 9, where it is seen that a percentage increase in f at a given Reynolds number over that for a smooth pipe is never accompanied by more than one-third the corresponding percentage increase in j_h, and usually the increase in j_h is even smaller. This agrees with the data of Sams (*25*) for square-thread-type roughness and with most of Cope's (*7*) data for pyramid-shaped roughness. In practice, the relatively small increase in heat transfer due to surface roughness will usually be negated by fouling, and so for design purposes the equations for a smooth pipe are recommended.

A replot of the heat transfer curves according to Equation (7*a*)

$$\frac{hD}{k_f}(Pr)_f^{-1/3} = aRe_f^{1-n} \qquad (7a)$$

is given in Figure 10. This method of plotting has the advantage of showing the heat transfer coefficient as a function of velocity, if pipe dimensions and fluid properties are assumed fixed, and allows comparison with the curves of both Cope and Sams. All the curves for the rough pipes in Figure 10 show a tendency to diverge from that for the smooth copper pipe at the higher Reynolds numbers. This divergence is again in agreement with the data of Sams but is at odds with those of Cope, who noted a tendency to converge at higher Reynolds numbers (*7*, *15*). The D/e ratios for the ⅛- and ¼-in. galvanized pipes are in the range of square-thread-type roughness ratios studied by Sams, and the heat transfer data are in substantial agreement. The Karbate pipe shows somewhat higher heat transfer coefficients at the lower Reynolds numbers than the other pipes. Such a tendency at the lower Reynolds numbers was also noted by Cope for his pyramid-roughened pipes, but not by Sams. Under a microscope, the surface of the Karbate pipe bore some resemblance to Cope's pipe-surface photographs. It appears, therefore, that although the steel and galvanized pipes behave more like square-thread-roughened pipes, the Karbate is closer to pyramid-shaped roughness.

At the lower Reynolds numbers, the steel and galvanized pipes show heat

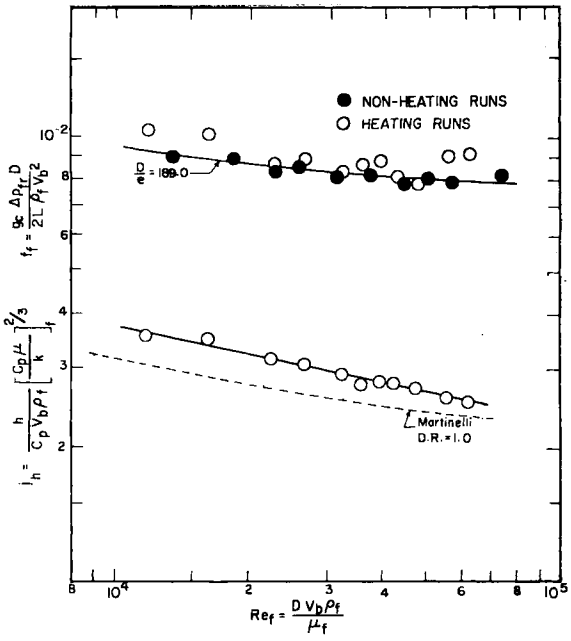

Fig. 6. Karbate pipe, 1/2 in.; fluid friction and heat transfer data.

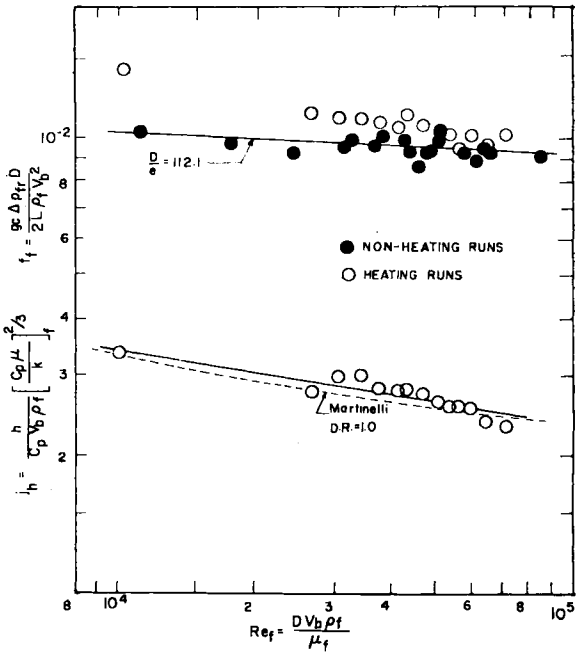

Fig. 7. Galvanized pipe, 1/4 in.; fluid friction and heat transfer data.

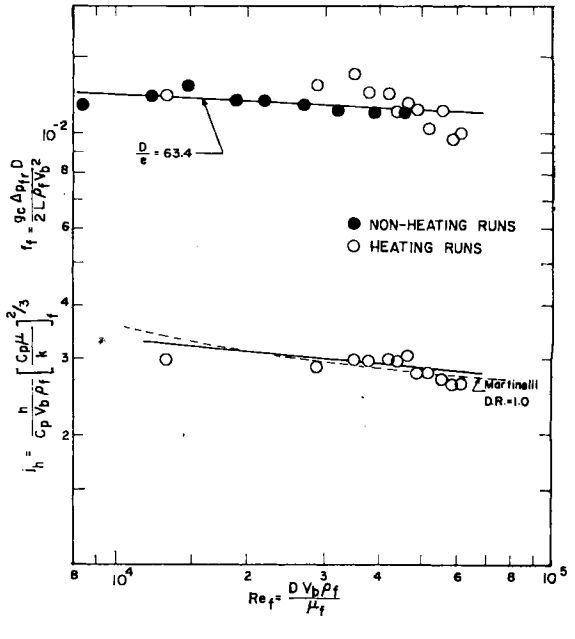

Fig. 8. Galvanized pipe, 1/8 in.; fluid friction and heat transfer data.

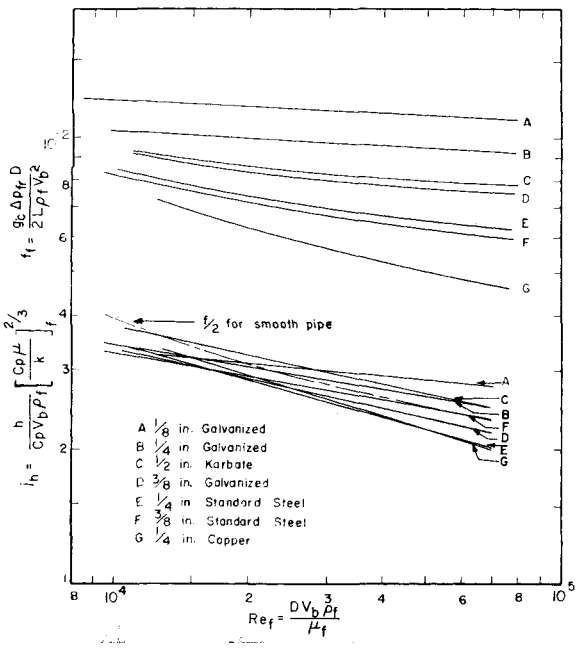

Fig. 9. Fluid-friction and heat-transfer curves for seven commercial pipes.

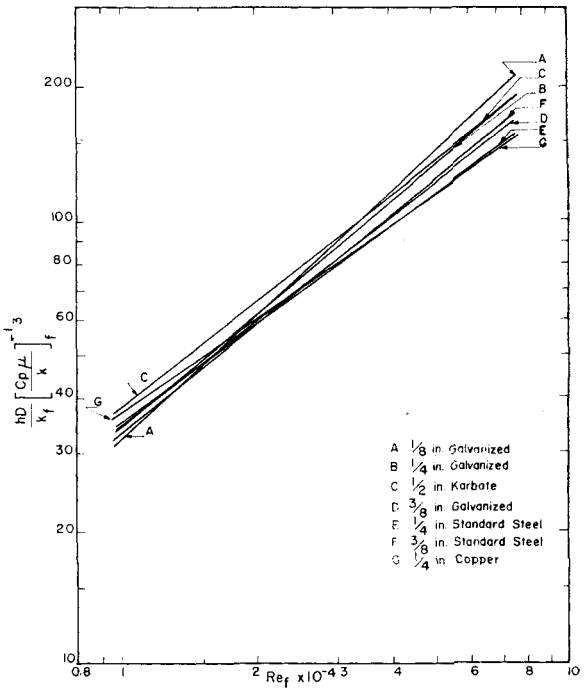

Fig. 10. Heat-transmission curves for *various pipes.*

transfer coefficients slightly smaller than for the smooth copper pipe, an effect also noted by Cope for one of his pipes, even lower in equivalent sand-roughness ratio D/e than that of the ⅛-in. galvanized pipe studied here. The possible experimental error for the lower velocity points in the case of the rougher pipes is, however, estimated to be as high as −10%, compared with an estimated average experimental error of −4% for all the runs. This decrease in accuracy for the low-velocity runs through the rougher pipes is primarily attributable to the considerably smaller exit terminal temperature differences measured for these runs and may account for the anomaly in the present investigation.

The dimensionless group j_h/f_fRe_f may be arranged as follows:

$$\frac{j_h}{f_fRe_f} = \frac{h}{\Delta p_{fr}} \cdot \frac{2L}{g_cD^2} \cdot \frac{\mu_f}{C_p\rho_f} \qquad (8)$$

For pipes of equal dimensions through which flow the same fluid at the same film temperature, the modulus j_h/Re_ff_f thus represents the relative heat transfer coefficients per unit pressure drop. This group is therefore used to compare heat-transmission performance of three pipes on a unit pressure drop basis, in Figure 11. It is apparent that over the entire range of Reynolds number studied, the smooth copper pipe is on this basis more efficient than the rougher Karbate pipe, which, in turn, is more efficient than the still rougher galvanized pipe. A similar result is shown in Figure 12, where the comparison is made on the basis of unit power loss with the modulus $j_h/Re_f^2f_f$. This group represents heat transfer coefficient per unit frictional power loss:

$$\frac{j_h}{f_fRe_f^2} = \frac{h}{\Delta p_{fr}V_b\frac{\pi}{4}D^2} \cdot \frac{\pi L}{2g_cD} \cdot \frac{\mu_f^2}{C_p\rho_f^2} \qquad (9)$$

As predictable, the differences between pipes on the unit power basis are somewhat smaller than on the unit pressure-drop basis.

MOMENTUM–HEAT TRANSFER ANALOGIES

The data on rough pipes offer a critical test of the many analogies between turbulent momentum and heat transfer which have been proposed.

Dealing with a turbulent system, and one in which Pr is near unity, Reynolds (*24*) originally argued that

$$j_hP_r^{-2/3} \qquad \frac{h}{C_pV\rho} = \frac{\alpha f}{2} \qquad (10)$$

The dimensionless constant α has commonly been taken as unity (*15, 18*). In the present study, for which Pr_f was essentially constant at 0.69, Equation (10) says that j_h is directly proportional to f. A similar result arises from Colburn's (*4*) empirical modification of the Prandtl-Taylor analogy:

$$j_h = \frac{f}{2} \qquad (11)$$

This proportionality between j_h and f, either at a fixed Reynolds number for varying roughness or for fixed roughness at varying Reynolds number, is at complete odds with the data of Figure 9. Equation (11) is suitable for smooth pipes, as in Figure 2, and is even applicable for approximate prediction of rough-pipe heat transfer if the f is for a smooth tube, as in Figure 9, but should not be applied when rough-pipe friction factors are used. Equation (10), with $\alpha = 1$, is a reasonable first approximation for pipes of intermediate roughness.

The equations of Taylor (*28*) and Prandtl (*22*), who developed the laminar sublayer concept, of von Kármán (*13*), who introduced the concept of a buffer layer between the laminar sublayer and the turbulent core, and of Pinkel (*21*), who based his work on the analyses of von Kármán and of Deissler (*9*), as well as on the empirical data of Sams (*25*), all lead in the present instance of a fixed Prandtl number to an equation of the form

$$j_h = \frac{\sqrt{f/2}}{b + c\cdot\sqrt{f/2}} \qquad (12)$$

where b is a constant which depends upon the Prandtl number and c is a constant which depends both on the Prandtl number and the wall roughness. Although Equation (12), unlike (10) and (11), does not imply direct proportionality between j_h and f at fixed Reynolds number, it does imply that where f becomes independent of Re for a rough pipe, j_h also becomes independent of Re. Reference to Figures 2 to 9 shows that this contradicts the experimental facts. After the friction factor curves for the rougher pipes have become practically horizontal, the j_h curves continue to slope downward. The artificial roughness data of Cope and of Sams show the same effect.

A momentum–heat-transfer analogy equation which does show a dependence of j_h with Re even after f has become independent of Re, is that developed by Boelter, Martinelli, and Jonassen (*2*) as

an extension of von Kármán's work. This was further refined by Martinelli (*17*) to include the effect of the diffusivity ratio D. R. Martinelli's equation, with equality of momentum and thermal eddy diffusivities assumed, may be written as

$$j_h = \frac{\sqrt{f/2}\,(Pr)^{2/3}\,\frac{\Delta t_{max}}{\Delta t_{mean}}}{5\left[Pr + \ln(1 + 5Pr) + 0.5\text{D.R.}\ln\frac{Re}{60}\sqrt{f/2}\right]} \qquad (13)$$

In the present instance no temperature profiles were measured and hence $\Delta t_{max}/\Delta t_{mean}$, which is a function of the radial temperature gradients, was not evaluated. However, since the density and other fluid properties have been evaluated at the "film" temperature, an empirical factor T_f/T_b has in effect been applied for handling such temperature gradients. If Pr_f is assigned its value for the present study 0.69, and if D.R. is taken as unity, Equation (13) reduces to

$$\frac{\sqrt{f_f}}{j_h} = 10.425 \cdot \log Re_f\sqrt{f_f} - 0.3395 \qquad (13a)$$

By use of the friction factor curves of Figures 2 to 8, plots of j_h vs. Re_f have been calculated according to Equation (13*a*) and are reproduced in the same figures. Agreement with the experimental data is good, particularly with several of the rougher pipes. Equation (13*a*) also indicates a straight-line relationship between $\sqrt{f_f}/j_h$ and $\log Re_f\sqrt{f_f}$. All the heating data were thus plotted in Figure 13, where again reasonably good agreement between the data and the Martinelli line occurs.

Except for the Karbate pipe, which, as already noted, displays its distinctive type of roughness, the greatest deviations between the experimental data and the Martinelli equation occur for the smoother pipes and for the lower Reynolds numbers, i.e., for low values of $Re\sqrt{f_f}$. These are precisely the points where the assumption of D.R. = 1.0 is in greatest error. Correct values of D.R. for these cases, since they are less than unity, would raise the Martinelli lines of Figures 2 to 8, particularly those for the smoother pipes at low Re.

A more rigorous test of the Martinelli equation with the present data is planned for the future. This will involve evaluation of D.R. by use of the formula developed by Martinelli (*17, 18*), accounting for radial temperature gradients by estimation and application of the factor $\Delta t_{max}/\Delta t_{mean}$, rather than by T_f/T_b, and applying the factor of Seban and Shimazaki (*26*) to convert the Martinelli derivation for uniform heat flux to the present case of uniform wall temperature.

Use of roughness Reynolds number and shear Stanton number as correlating parameters is currently under trial.

ACKNOWLEDGMENT

The authors are indebted to the National Research Council of Canada and to the U.B.C. President's Committee on Research for grants-in-aid of this study. Thanks are also due to B. C. Almaula, who initiated the construction of the apparatus.

NOTATION

- a = constant in Equation (7), dimensionless
- a.d. = average deviation between measured j_h and j_h calculated by Equation (7), %
- b = constant in Equation (12), dimensionless
- c = constant in Equation (12), dimensionless
- C_p = heat capacity of fluid, B.t.u./(lb.)(°F.)
- D = inside diameter of pipe, ft.
- D.R. = diffusivity ratio = $E_H/(E_H + k/\rho C_p)$, dimensionless
- e = equivalent sand roughness, ft.
- E_H = eddy diffusivity of heat, sq. ft./hr.
- f = Fanning friction factor, $\Delta p_f D g_c/2LV^2\rho$, dimensionless
- g_c = conversion factor = 4.17×10^8 (lb.)(ft.)/(hr.)^2(lb.-force)
- G = mass velocity, lb./(hr.)(sq. ft.)
- h = coefficient of heat transfer between fluid and surface, B.t.u./(hr.)(sq. ft.)(°F.)
- j_h = heat transfer factor = $(h/C_pV\rho)(Pr)_f^{2/3}$

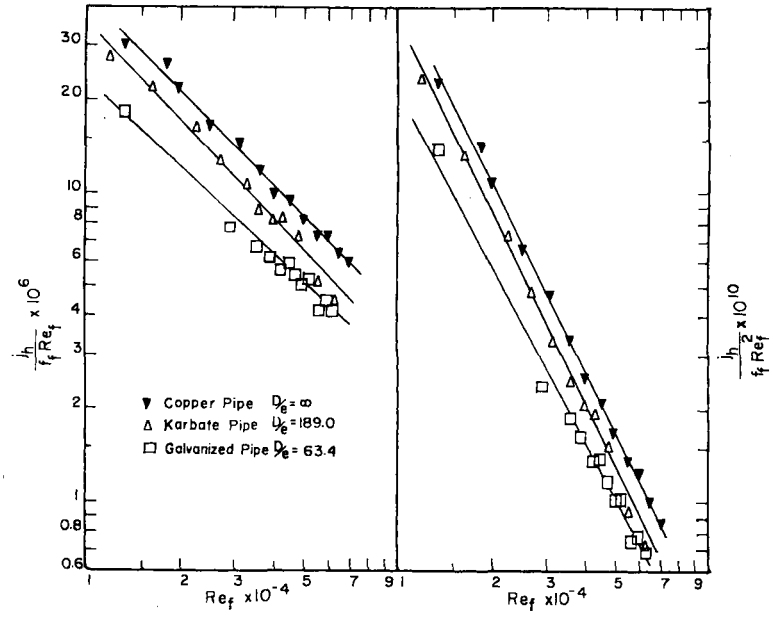

Fig. 11. Heat transmission per unit pressure drop for three pipes.

Fig. 12. Heat transmission per unit power loss for three pipes.

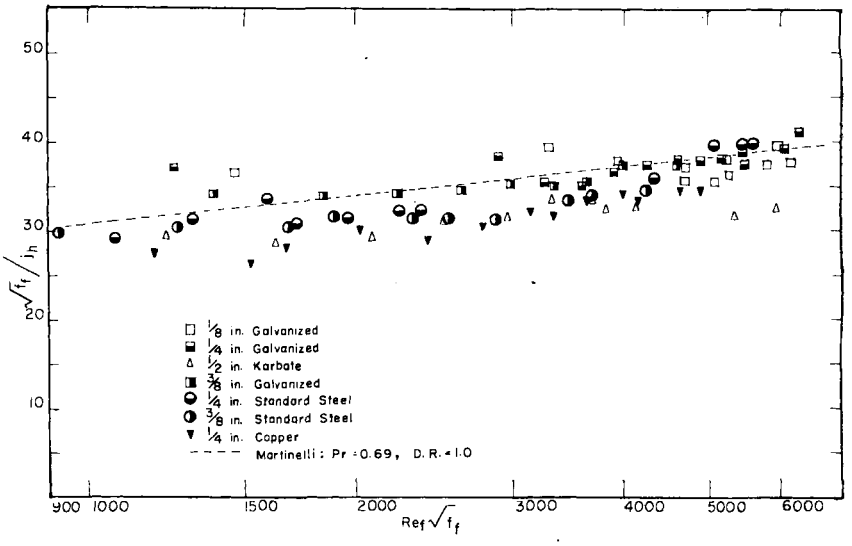

Fig. 13. Test of Martinelli's analogy.

k = thermal conductivity of fluid, (B.t.u.)(ft.)/(hr.)(sq. ft.)(°F.)
L = length of pipe, ft.
n = constant in Equation (7) = slope of j_h vs. Re_f curves in Figure 9 = 1 − slope of curves in Figure 10, dimensionless
p = absolute pressure, lb.-force/sq. ft.
Δp_{fr} = frictional pressure drop, lb. force /sq. ft.
Pr = Prandtl number = $C_p\mu/k$, dimensionless
Re = Reynolds number = $DV\rho/\mu$, dimensionless
t = temperature of fluid, °F.
t_b = average bulk temperature of fluid = $(t_1 + t_2)/2$, °F.
t_f = film temperature = $(t_b + t_s)/2$, °F.
t_s = inside surface temperature of pipe, °F.
Δt_{max} = temperature difference between inside surface of pipe and axis of pipe, °F.
Δt_{mean} = temperature difference between inside surface of pipe and bulk of fluid, °F.
T = absolute temperature, °R.
V = velocity of fluid, ft./hr.
V_b = velocity of fluid defined by G/ρ_{avg}
v = specific volume of fluid, cu. ft./lb.
w = weight rate of air flow, lb./hr.
α = ratio of total diffusivity of heat to total diffusivity of momentum, dimensionless
μ = viscosity of fluid, lb./(ft.)(hr.)
ρ = density of fluid, lb./cu. ft.
ρ_{avg} = density of fluid evaluated at $(p_1 + p_2)/2$ and t_b, lb./cu. ft.
ρ_f = density of fluid evaluated at $(p_1 + p_2)/2$ and t_f, lb./cu. ft.

Subscripts

1 = test pipe entrance (slightly different for pressure drop than for heat transfer)
2 = test pipe exit (slightly different for pressure drop than for heat transfer)
b = bulk, evaluated at temperature t_b
f = film, fluid properties evaluated at temperature t_f

LITERATURE CITED

1. Am. Soc. Mech. Engrs., "Rept. of A.S.M.E. Special Research Committee on Fluid Meters," 4 ed. (1937).
2. Boelter, L. M. K., R. C. Martinelli, and Finn Jonassen, *Trans. Am. Soc. Mech. Engrs.*, **63**, 447 (1941).
3. Boelter, L. M. K., C. Young, and H. W. Iversen, *Natl. Advisory Comm. Aeronaut. Tech. Note* 14-51 (1948).
4. Colburn, A. P., *Trans. Am. Inst., Chem. Engrs.*, **29**, 174 (1933).
5. ——— *Purdue Univ. Eng. Bull. Research Ser.*, **84**, p. 52 (1942).
6. Colebrook, C. F., *J. Inst. Civil Engrs.*, 11, 133 (1938-39).
7. Cope, W. F., *Proc. Inst. Mech. Engrs.*, **145**, 99 (1941).
8. Chu, H., and V. L. Streeter, Ill. Inst. Technol. *Proj.* 4918 (Aug. 1949).
9. Deissler, R. G., *Trans. Am. Soc. Mech. Engrs.*, **76**, 73 (1954).
10. Drexel, R. E., and W. H. McAdams, *Natl. Advisory Comm. Aeronaut. Wartime Rept.* 108 (1945).
11. Humble, L. V., W. H. Lowdermilk, and L. C. Desmon, *Natl. Advisory Comm. Aeronaut. Rept.* 1020 (1951).
12. Kármán, T. von, *Natl. Advisory Comm. Aeronaut. Tech. Mem.* 611 (1931).
13. ———, *Trans. Am. Soc. Mech. Engrs.*, **61**, 705 (1939).
14. King, W. J., and A. P. Colburn, *Ind. Eng. Chem.*, **23**, 919 (1931).
15. Knudsen, J. G., and D. L. Katz, "Fluid Dynamics and Heat Transfer," p. 177, Univ. Mich. Press, Ann Arbor (1954).
16. Latzko, H., *Natl. Advisory Comm. Aeronaut. Tech. Mem.* 1068 (1944).
17. Martinelli, R. C., *Trans. Am. Soc. Mech. Engrs.*, **69**, 947 (1947).
18. McAdams, W. H., "Heat Transmission," 3 ed., McGraw-Hill Book Company, Inc., New York (1954).
19. Nagaoka, J. and A. Watanabe, *Proc. 7 Intern. Congr. Refrig., The Hague-Amsterdam*, **3**, No. 16, 221 (1937).
20. Nikuradse, J., *Forschungsheft*, **361**, 1 (1933).
21. Pinkel, Benjamin, *Trans. Am. Soc. Mech. Engrs.*, **76**, 305 (1954).
22. Prandtl, L., *Physik, Z.*, 11, 1072 (1910); **29**, 487 (1928).
23. Pratt, H. R. C., *Trans. Inst. Chem. Engrs. (London)*, **28**, 177 (1950).
24. Reynolds, Osborne, *Proc. Manchester Lit. Phil. Soc.*, **14**, 7 (1874).
25. Sams, E. W., *Natl. Advisory Comm. Aeronaut. Research Mem.* E52 D17 (1952).
26. Seban, R. A., and T. T. Shimazaki, *Trans. Am. Soc. Mech. Engrs.*, **73**, 803 (1951).
27. Sherwood, T. K., and C. E. Reed, "Applied Mathematics in Chemical Engineering," 1 ed., McGraw-Hill Book Company, Inc., New York (1939).
28. Taylor, G. I., *Brit. Advisory Comm. Aeronaut. Rept. and Memo.* 272 (1917).
29. Tribus, Myron, and L. M. K. Boelter, *Natl. Advisory Comm. Aeronaut. A.R.R.* (Oct. 1942).

Presented at A.I.Ch.E. Boston meeting

Control of Continuous-flow Chemical Reactors

OLEGH BILOUS, H. D. BLOCK, and EDGAR L. PIRET

University of Minnesota, Minneapolis, Minnesota

I. Frequency-response Relations for a Continuously Stirred Tank Reactor

Although applications of frequency-response techniques to the control of processes are well known in electrical engineering and in the instrumentation field, relatively little has been done to develop in a quantitative manner the employment of these techniques in the control of chemical reactions. As a result the control characteristics of chemical reactors are today being come upon either in the pilot plant or in the field. This study was motivated by the fact that processes designed on the basis of steady state operation may sometimes prove inadequate for automatic control.

Olegh Bilous is with Laboratoire Centrale des Poudres, Paris, France, and H. D. Block at Cornell University, Ithaca, New York.

It is the purpose of this paper then to show how frequency-response analysis may be used to develop the theory of control of continuous-flow chemical reactors. The response equations are developed for simple and complex reactions of any order, and, for clarity, their applications are illustrated with selected numerical examples and by the use of polar plots.

The effects on the reactor-product stream which are considered in the equations include variations in feed-stream composition and temperature, the heat input or cooling of the reactor by coils, and the effect of temperature level on the rates of reaction and of heat release. How automatic-control requirements may influence proper reactor design is also illustrated. Only single-stage reactors are considered here. Chains of reactors will be treated in Part II.

The transient behavior of continuous reactor systems has been considered by Mason and Piret (*7*) and the self-regulation properties of chains of reactors by Devyatov and Bogshev (*3*); Kramers and Alberda (*6*) have applied the method of complex amplitudes to the study of mixing and residence times in reactors. These investigations are all limited to first-order processes with no temperature effects. Transient equations for second-order processes in continuous reactors with no temperature effects were recently treated by Acton and Lapidus (*1*). The